Cooperation of partially-transformed clones: the invisible force behind the early stages of carcinogenesis

Alessandro Esposito

The Medical Research Council Cancer Unit, University of Cambridge, Hills Road, Cambridge CB2 0XZ, UK

Correspondence should be addressed to A.E. (email: ae275@mrc-cu.cam.ac.uk)

Running title: Oncogenic field effect and clonal heterogeneity

Keywords: oncogenesis, non-cell-autonomous, model

Abstract

Early models and observations on the clonal origin of cancer asserted that cancer arises from a sequence of rare mutations that confer the capability to one cell, and its progeny, to grow outside the control of the tissue of origin. More recently, theories for polyclonal tumour evolution and accumulating experimental evidence have challenged this perspective. However, the role and a model for non-cell-autonomous mechanisms during mutationally-driven carcinogenesis, at the best of our knowledge, are not well characterised. Therefore, we developed a simple yet insightful theoretical framework to address the question of how frequent and important non-cell-autonomous mechanisms during the early steps in carcinogenesis might be. We show that the three-dimensional tissue architecture is likely to amplify local non-cell-autonomous mechanisms of carcinogenesis mediated by cooperation of different, non- or partially- transformed mutants. We thus propose that clonal cooperation during the earliest steps in oncogenesis is an under-appreciated process, yet a phenomenon that might be an essential force that shapes tumour evolution.

Introduction

The cooperation between tumour cells and its environment and the competition between different tumour clones during carcinogenesis are well-established[1]. Other types of cooperations, for instance, the positive cooperation between tumour clones, or even non-transformed clones, have been increasingly recognised as a possible fundamental driving force in cancer as well[2, 3]. The complexity of all possible clonal interactions, particularly during the late stages of cancer, is, therefore, fostering research aimed to model cancer from an ecological perspective[1, 4]. Already in the nineties, Tomlinson and Bodmer modelled fitness advantage in angiogenesis, where a tumour clone may benefit others[2]. The possibility that partially transformed tumour cells might cooperate was then explicitly generalised by Axelrod and colleagues[3]. Furthermore, several recent experimental findings suggest a significant role for both cooperation and polyclonality in the emergence of cancer.

Glioblastoma multiforme tumours, for instance, exhibit considerable intra-tumoral heterogeneity including the pathogenic expression of an oncogenic truncation of the epidermal growth factor receptor (ΔEGFR) gene and EGFR amplification[5]. The less frequent ΔEGFR clones are capable to support an increase fitness of the more prevalent cells overexpressing EGFR, through secretion of IL6 and LIF and a paracrine effect. Recently, Reeves and colleagues[6] have used multi-colour lineage tracing with a Confetti mouse line together with the topical administration of a carcinogen, to study clonal evolution during early oncogenesis. Interestingly, the authors observed benign papillomas harbouring a HRAS Q61L mutation with streaks of Notch mutant clones. Although these Notch mutants were considered infiltrating clones with no active role in the oncogenic process, Janiszewska and Polyak[7] noted that cooperation between the Notch and HRAS mutants could not be excluded and that streaks of Notch clones are reminiscent of structures found in non-mutualistic colonies of buddying yeast. Although unproven, it is conceivable that the less frequent clones can provide, altruistically, a fitness advantage to the HRAS mutant cells similarly to what has been observed for glioblastoma multiforme[5, 8] or for Wnt-secreting wild-type HRAS clones supporting HRAS mutants[9]. While facilitating the oncogenic process, a non-mutualistic clone would be then outcompeted by more aggressive clones after a clonal sweep and diversification into multiple intermixed mutants[6] suggestive of mutualistic clonal interactions[7].

However, it is unclear if these observations, often obtained using model systems with carcinogens or established tumour clones, can be recapitulated at the low mutational rates occurring naturally[10]. Furthermore, it is unknown at which stage of carcinogenesis, non-cell-autonomous mechanisms might have a role[9]. Therefore, the question addressed in this work is not *if* cooperation between mutant (partially-transformed) cells can occur, but *how likely* or *when* distinct mutations can occur in different cells cohabiting within the same tissue. We develop a simple and yet powerful model in the attempt to answer these fundamental questions. We propose that the extremely low mutational frequency encountered in physiological conditions does not render cooperation between mutations in adjacent cells unlikely but – rather the opposite – that synergy between the mutational process and cell-to-cell communication might play a fundamental role in carcinogenesis.

Results

A model for mutationally-driven cooperation in oncogenesis. We aim to develop the simplest possible model to address the very basic question of how likely mutationally and non-cell-autonomous driven polyclonal carcinogenesis is. We consider a low mutational rate ρ_0, constant throughout oncogenesis and equal for each possible oncogenic mutation[11]. With oncogenic mutation, we refer to any mutation that at any given time (not necessarily when it occurs) might contribute to the increased fitness of a clone that will eventually evolve into cancer, either through cell-autonomous or non-cell-autonomous mechanisms.

The probability for a single cell to accrue two specific mutations independently within a given time-interval is thus p_0^2 (with $p_0 = \rho_0 t << 1$). The probability that two neighbouring cells exhibit one given mutation each independently is, unsurprisingly, the same. Initially, we assume non-dividing cells in a well-organised tissue that after accumulating these two mutations acquire a fitness advantage. We will refer to these cells as initiated or transformed, but we will use these terms very loosely only to indicate a gain in fitness.

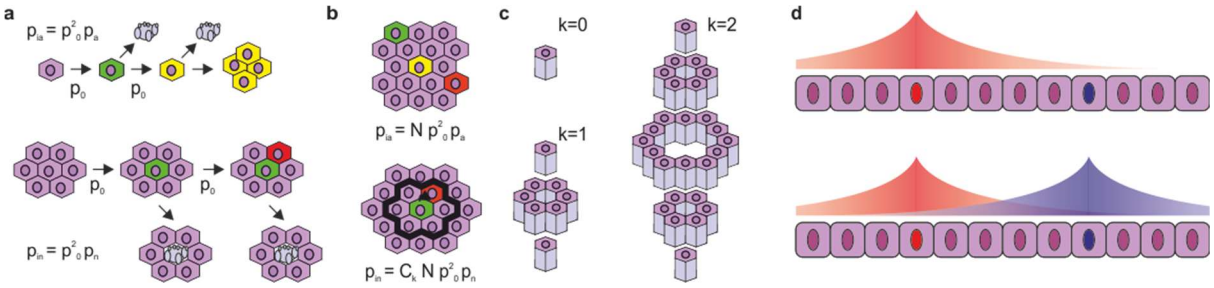

Figure 1 | Tissue organisation and non-cell-autonomous mechanisms. ***a****) A simple model where cells accumulate two mutations (top) or two mutations occur in different cells within the same neighbourhood (bottom).* ***b****) When the probability to accrue mutations is low, within tissue of N cells, there will be more opportunities for mutations to co-occur within a given neighbourhood (bottom) rather than within the same cell (top).* ***c****) The neighbourhood of a cell can be described as a problem of geometrical tessellation of space which will depend on tissue organisation, here shown a simple example of hexagonal pillars tesselating space.* ***d****) gradients of shared resources (e.g., growth factors or metabolites) might be then induced by either one or the other cell triggering interactions by juxtacrine or paracrine effects.*

In tissue with N cells, the probability of cell-autonomous initiation of one mutant cell is simply $p_{ia}=Np_0^2p_a$. Similarly, the probability of non-cell-autonomous initiation is $p_{in}=NCp_0^2p_n$. p_a and p_n are defined as the probabilities that one cell harbouring the right pair of mutations – either

by itself or within its neighbourhood – survives tumour suppressive mechanisms (**Fig. 1a**). C is a coordination number, *i.e.* the number of cells within the neighbourhood of a reference cell (**Fig. 1b, c**). Within the validity of common assumptions (*e.g.*, equally probable, spatiotemporally-invariant and independent mutational events), the probability of initiation within a group of N cell is the sum of p_{ia} and p_{in}: $p_i = Np_0^2 p_a(1 + \Omega p_{n0}/p_a)$ with $\Omega = Cp_n/p_{n0}$ and where p_{n0} is the probability that one cell is transformed when directly in contact with another mutant.

p_n (and thus Ω) depends on tissue organization and the type of cell-to-cell cue that contributes to the process of transformation (**Fig. 1d**). With this simple notation, the answer to our central question can be thus separated into the study of tissue organization (the factor Ω) and the magnitude of p_{n0} compared to p_a.

Tissue organisation. To model the organisation of tissue wherein mutated cells are resident, several aspects of tissue organisation have to be considered:

i) the more distant a neighbouring cell is, the lower the probability of cooperative non-cell-autonomous effects should be, *i.e.* p_n shall be a function of distance;
ii) *C* is the sum of cells in extended neighbourhoods or the sum of C_k, *i.e.*, the number of cells in the k-neighbourhood, where k=1 defines cells in contact;
iii) C_k depends on tissue architecture that we model as a problem of three-dimensional tessellations of space;
iv) tissues are compartmentalised and, therefore, boundaries effects should be considered.

For convenience, we describe C_k just for two different tissue topologies, a tissue organised in stacked hexagonal pillars or a thin layer of similar hexagonal pillars. In the former case, cells tessellate a three-dimensional space and we neglect effects at the periphery. In other words, we assume that the number of cells contained within a tissue is larger than the cells at its periphery. **Fig. 1** illustrates the progression of the number of cells included in subsequent neighbourhoods. In **Appendix 1** we demonstrate that $C_k = 6k^2+2$. For a significantly more constrained topology where only three layers exist $C_1 = s_0 + 2$ and $C_{k>1} = s_0(3k - 2)$. This description permits us to evaluate analytically the effects of tissue organisation on the probability of cooperation between mutations. In the next section, we provide also numerical examples showing the general validity of this model in the presence of even more stringent topological constrains.

Oncogenic field effect. Without loss of generality, we assume that the interaction between two mutant cells is mediated by a sharing diffusible product[3], for instance a growth factor or a metabolite. Eldar *et al.* have modelled how the concentration of a signalling molecule (a morphogen) secreted by a cell decays in space[12]. Typically, the morphogen concentration is abated by passive diffusion and linear degradation resulting in exponentially decaying concentration gradients. However, ligand-morphogen interactions can induce non-linear mechanisms of morphogen degradation resulting in power-law decays. Therefore, here we model the decay of an oncogenic field akin morphogen gradients using power or exponential decays because of their physiological relevance[12-14].

For the case of a power function ($p_n(k) = p_{n0}\, k^{-l}$) and a three-dimensional tissue described by hexagonal pillars ($C_k = 6k^2+2$), the factor Ω can be described analytically with $\Omega(l) = 6\zeta(l-2) + 2\zeta(l)$ as demonstrated in **Appendix 2**. ζ is the Riemmann Zeta function and is finite only for an argument larger than one (here l-2>1). Therefore, for a large interconnected tissue, oncogenic biochemical gradients induced by a mutant cell must decay very steeply for non-cell-autonomous mechanisms not to dominate. In the limiting case where only the 1-

neighbourhood is relevant for transformation ($l \to \infty$), the Riemann Zeta function converges to unity and therefore $\Omega = 8$. This is just the number of cells in direct contact to the reference cell (C_1) showing mathematical consistency and providing a lower boundary to Ω in the case of small effects in a very constrained topology. Conversely, for shallower gradients where the Riemann Zeta function does not converge (l<4), these probabilities will be significantly larger. We obtained these results modelling tissues of non-finite extensions to derive analytical solutions. However, through numerical estimations, it is simple to demonstrate how these observations are generally valid and correct also for small volumes of cells (**Fig. 2a-b**). For example, in a small neighbourhood with a radius of 10 cells, Ω ~ 11.5 (l=4) and Ω ~ 340 (l=1), values that reach 12 and 3 10^4, respectively, for a neighbourhood with a radius of 100 cells.

Similarly, in **Appendix 2** we demonstrate that for a thin three-layer tissue, $\Omega = 12\zeta(l-1) - 8\zeta(l) + 4/3$. This series converge for l>2 and for l=3, Ω = 11.7 and numerical estimations (**Fig. 2a**) show that Ω reaches values of ~24 and ~50 for l=2 within a limiting neighbourhood with a 10 or 100 cell radius, respectively. In the limit case where only the first neighbourhood is relevant ($l \to \infty$), Ω ~ 5.3. Therefore, even within this rather constrained topology, Ω obtains rather large values. However, gradients described by power functions are shallower than exponentially decaying gradients at longer distances. Although both gradients are physiologically relevant, power-like functions might overestimate Ω. The formalism for exponentially decaying oncogenic fields is less elegant (see **Appendix 3**); however, it can be readily demonstrated that even for steep gradients decaying of a third at every cell distance (k_c=1), Ω can assume double-digit values (see also **Fig. 2b**).

Therefore, basic mathematical and topological principles suggest that cell-to-cell interactions within a tissue, here described by the magnitude of Ω (the oncogenic field effect), must significantly contribute to tumorigenesis.

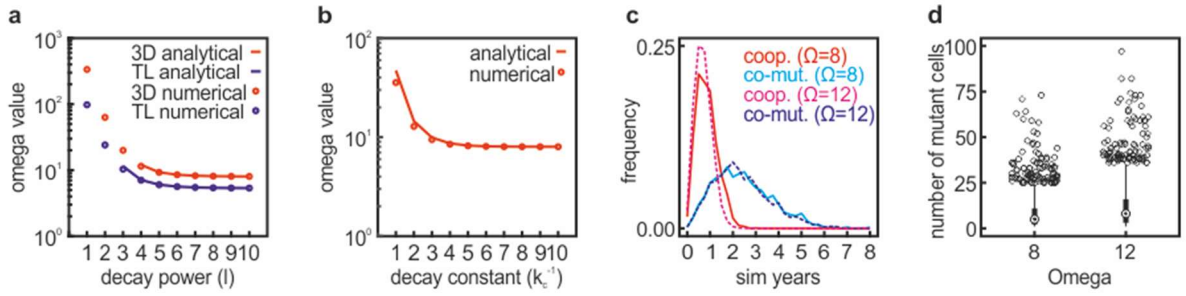

Figure 2. Numerical validation of the oncogenic field solutions and cell-autonomous time-horizon. ***a****) Comparison between numerical and analytical solutions to estimate the value of the oncogenic field factor Ω for a three-dimensional (red, 3D) and three-layered (blue, TL) tissue model. The solid lines represent the analytical solutions within the limits of its convergence (l>2 for TL and l>3 for 3D). The numerical estimations, computed over a small 10-cell radius neighbourhood, confirms the observations we reported, more generally, on the analytical solutions, including the necessity of steep power decays and a convergence to Ω~8 (3D) and Ω~5.3 (TL) for these limiting cases.* ***b****) Identical computations described in a) but for the exponential decay model for a three-dimensional tissue. Both the analytical solution and numerical estimates converge to the value of Ω~8 for steep decays. The analytical approximations provide larger values for Ω for shallow decays, without changing the interpretation of the proposed model.* ***c****) Distribution of waiting times for the occurrence of two co-occurring mutations (blue) or for cooperating mutations through non-cell-autonomous mechanisms (red) in the limiting case of cells in contact (Ω~8) and for Ω~12. As predicted, the median of the two distributions scales as* $\sqrt{\Omega}$. ***d****) Distribution of the number of clones cooperating through non-cell-autonomous mechanisms at the time of appearance of mutants with two mutations.*

Cell-autonomous time-horizon. So far, we have discussed *if* and *how likely* mutationally-driven non-cell-autonomous mechanisms are; next, we address the question about *when* these mechanisms are more likely to occur. Indeed, we have demonstrated that non-cell-autonomous mechanisms can increase the probability that mutations contribute to carcinogenesis by a factor Ω. A corollary to this observation is that non-transformed cells might contribute to tumour initiation earlier than cell-autonomous mechanisms. When we consider only the mutational process (*i.e.*, neglecting p_a and p_{n0}), one cell accrues pairs of mutations at the rate ρ_0 but within a neighbourhood cells accrue mutations at an apparent rate of $\rho_0\sqrt{\Omega}$. This simple mathematical inference is confirmed by Monte Carlo simulations (see **Fig. 2c-d** and **Methods** - ρ_0=10^{-6} mutations/day, N=10^6 cells, 2,000 replicates) showing that the median time of appearance for a double-mutant cell is ~27 months, while cooperating cells with single mutations first appear at a median time of 8-10 months ($\Omega = 12$ or 8, respectively; **Fig. 2c**). In first approximation, the average time t_a for a tissue of N cells to accrue two mutations will be inversely proportional to ρ_0N. t_a, the time-horizon after which cell-autonomous mechanisms might dominate, is preceded by a latency period during which only single mutations are likely. This latency period is followed by a significantly long period $t_a\Omega^{-0.5} \leq t < t_a$ when mutationally-driven cooperation between adjacent cells is more likely than mutationally-driven cell-autonomous mechanisms. For instance, in the limiting case where only the first-neighbourhood significantly contribute to tumour initiation ($\Omega = 8$), during 65% of the time interval preceding t_a, clonal cooperation is likely to be a fundamental mechanism that synergizes with the mutational process to support partially transformed clones. In support of this observation, results from Monte Carlo simulations show that at the time of appearance of the first clone with two co-occurring mutations, ~20% of simulations did not detect co-operating clones. However, the remainder ~80% of cases exhibit co-operating clones at the time of appearance of the first double-mutant even when a very conservative case of $\Omega = 8$ is considered (**Fig. 2d)**.

The mathematical model we present here is simple but useful to highlight the possibility that non-cell-autonomous mechanisms might dominate in the early stages of carcinogenesis. Once a proliferative tissue is considered, with a fitness advantage for cooperative clones compared to wild-type cells, the presence of these non- or partially- transformed clones would be even more significant, increasing the probability to accrue further mutation at a faster pace and shaping the initial period of oncogenesis.

Discussion

A role for non-cell-autonomous mechanisms in cancer is well-established, often as mechanism of interaction between cancer cells and the surrounding tissue[2, 15-18]. The cooperation of non- or partially- transformed clones as a driving force underling oncogenesis has been also hypothesized[3], and there is nowadays accumulating evidence suggesting that a description of oncogenesis focused exclusively on cell-autonomous mechanisms might under-represent the importance of oncogenic signalling in cancer[5, 9, 18].

Experiments in *Drosophila melanogaster* have also shown that inter-clonal cooperation between mutants harbouring an oncogenic KRAS mutation or inactivation of the tumour suppressor *scrib* can support tumorigenesis mediated by JNK and JAK/STAT signalling[19]. Recently, Marusyk and colleagues (2014) have used a mouse xenograft model to test the effects of clonal heterogeneity demonstrating that clones expressing the chemokines IL11 are capable to stimulate overall tumour growth through a non-cell-autonomous mechanism, while clonal interference maintains genetic intra-tumour heterogeneity[9]. Similarly, Inda and

colleagues (2010) have shown how intra-tumour heterogeneity observed in glioblastoma can be maintained through cross-talk between mutants harbouring a ΔEGFR that secrete IL6 and LIF to support fitness in clones with EGFR amplification[5]. Clearly and colleagues (2014) has also shown that Wnt-producing HRAS wild-type clones can support tumorigenicity and clonal heterogeneity by cooperating with clones harbouring mutant oncogenic HRAS[20]. These observations support the emerging notion that intra-tumoral heterogeneity is often of polyclonal origin and is an active process supported by non-cell-autonomous mechanisms. However, the role for poly-clonality and clonal cooperation during the early steps in oncogenesis is occasionally seen in contradiction with the low estimates of mutational rates in cancer[10]. Furthermore, it is unclear if clonal cooperation has a role during early oncogenesis or only at later stages when an heterogeneous tumour is established[20].

Aiming to contribute filling this gap in knowledge, we developed a simple model for the study of the basic principles of cooperation between the mutational process and cell-to-cell communication. Our analysis rise provoking observations on the earliest steps in oncogenesis. We show that irrespectively of the background mutational rate, if a set of transforming mutations are sufficiently likely to occur within a single cell in the lifetime of a patient, an equally rare yet oncogenic set of mutations are equally (or more) likely to contribute to tumorigenesis through non-cell-autonomous mechanisms. We have introduced the parameter Ω which capture the impact of tissue organisation and non-cell-autonomous mechanisms on cancer evolution. We modelled non-cell-autonomous mechanisms in analogy to morphogens during embryonic developments. Ω describes the magnitude with which paracrine, juxtacrine and other mechanisms mediated by shared substrates (*e.g.*, growth factors and metabolites) might impact transformation of a cell or clone. As such, Ω represent an oncogenic field effect, where oncogenic fields have the opposite outcome of morphogens by contributing to the de-regulation of tissue homeostasis. Furthermore, we have identified a stage of oncogenesis during which clonal cooperation might not simply coexist with clonal competition but even dominate before the emergence of clones capable of growing autonomously.

With the help of our model, experimentally, the problem is reduced to the measurement of quantities such as p_{n0} and p_a or the abundance of genes that, once mutated, can drive oncogenesis by non-cell-autonomous mechanisms. We argue that the magnitude of the oncogenic field effect (Ω) and the prediction of an autonomous time-horizon ensure a significant role for mutationally-driven and non-cell-autonomous mediated poly-clonal evolution of cancer during, at least, a very early stage of oncogenesis. Oncogenic field effects might be further amplified in tissues by compartmentalisation, abrogated by diffusion into lumens or the vascular system, or might be affected by systemic alterations of shared resources (*e.g.*, hormones, lipids). Our model highlights the importance of identifying the genes and the shared resources that can mediate clonal cooperation, such as growth factors (*e.g.*, mitogens, interleukins, *etc.*) or even metabolic by-products that are often at the basis of cooperative behaviour in lower organisms[21-23].

The theory described here was aimed to be simple and, at the best of our knowledge, it is a first attempt to describe the problem with an explicit mathematical model to extend the existing models of oncogenesis to non-autonomous mechanisms. Indeed, we emphasise that our model is not in contradiction with the prevailing models of oncogenesis, as it is based on similar assumptions, but it highlights an equally important role for tissue organisation and cell-to-cell communication that cooperate synergistically with a mutationally driven processes.

Methods

The mathematical demonstration of the analytical equations presented in this work are described in **Appendices 1-3**.

The numerical evaluation of these analytical results (**Fig. 2a-b**) were performed with the Matlab script '*analytical_and_numerical_comparisons'* (Mathworks, version 2018) freely available from the GitHub repository *alesposito/CloE-PE*. The numerical estimations simply compare the value obtained from the approximated analytical solutions described in the appendices to direct numerical estimate computed on given neighbourhoods with features described in the main text.

Thee Monte Carlo simulations (**Fig. 2c-d**) used to evaluate the relationship between the time-horizon for cell-autonomous mechanisms (t_a) and non-cell-autonomous mechanisms are available as the Matlab script '*polyclonal_mutation_cooccurence_check'* freely available from the GitHub repository *alesposito/CloE-PE*. Briefly, we simulated a lattice of 10^6 cells with a mutational rate equal to 10^{-6} mutations per cell per simulated day (simday). At each simday, a random number generator was used to determine if and which of four independent mutations (A, B, C and D) occurred. When a cell acquires both A and B mutations, an AB-mutant cell is established. When a D mutation appears in a given neighbourhood of a C-mutant, a CD-cooperative cloned is logged. As soon as at least one AB- and one CD- clones are established, the simulation is interrupted. Simulations are then repeated 2,000 times and distributions of appearance of first AB- or CD- clones, and number of CD- clones at the appearance of an AB- clone generated.

The scripts were run on a Dell Precision 5810 workstation utilizing an Intel Xeon E5-1625 CPU and 64GB RAM.

Acknowledgments

A.E. acknowledges financial support provided by the Medical Research Council (UK) through a core grant to Prof. Ashok Venkitaraman.

Supporting information

Appendix 1 – Description of tissue organization. The 1-neighbourhood of an individual cell will contain 6 adjacent cells within the plane and 2 polar cells, one at the top and one at the bottom of the reference cell. The 2-neighbourhood will contain 12 cells within the plane, 6 cells in the above and bottom layers and two polar cells. The 3-neighbourhood will have 18 cells within the plane, 24, 12, 6 and 2 in the other layers. By induction, we infer that the k-neighbourhood of an individual cell in such tessellation is made of ks_0 cells within the plane, the sum of is_0 for each of the above and below layers where I will be form i=1 to k-1 and the two polar cells:

$$C_k = ks_0 + 2\sum_{i=1}^{k-1} is_0 + 2$$

To simplify, ks_0 (s_0 here is 6) can be brought within the sum, then allowing to simplify to the correspondent triangular number:

$$C_k = -ks_0 + 2\sum_{i=1}^{k} is_0 + 2 = k^2 s_0 + 2$$

It should be noted that for intercalated layers, the coordination values can be larger.

Another example, this time including a significant constrain in topology, is represented by the same topology, where only three layers are considered.

$$C_1 = s_0 + 2$$

$$C_{k>1} = ks_0 + 2(k-1)s_0 = s_0(3k-2)$$

Appendix 2 – Probability of initiation (power function). Let's assume the probability of tumour initiation is proportional to a concentration gradient, similar to a morphogen, or an oncogenic mitogen/morphogen field decaying as a power function:

$$p_{nk} = \frac{p_{n0}}{k^l}$$

Where p_{n0} indicate the probability of tumour initiation when cells are attached (the 1-neighbourhood). Therefore, in the case of 3D hexagonal tessellation, the we can now derive the factor Cp_n:

$$\Omega = \sum_{k=1}^{\infty} \frac{k^2 s_0 + 2}{k^l}$$

This sum is carried over an infinite neighbourhood and the validity of the results will be checked numerically. First we can expand p_{tn}:

$$\Omega = s_0 \sum_{k=1}^{\infty} k^{2-l} + 2\sum_{k=1}^{\infty} k^{-l}$$

These series can now be described by Riemann Zeta functions:

$$\Omega = s_0 \zeta(l-2) + 2\zeta(l)$$

Let's now consider the thin 3-layer tissue which tessellation was already discussed. In this case, for one cell:

$$\Omega = s_0 + 2 + \sum_{k=2}^{\infty} \frac{s_0(3k-2)}{k^l} = 2 + \sum_{k=1}^{\infty} \frac{s_0(3k-2)}{k^l}$$

Following the same process, we have described before, we can obtain:

$$\Omega = 2 - 2s_0 \sum_{k=1}^{\infty} \frac{1}{k^l} + 3s_0 \sum_{k=1}^{\infty} \frac{1}{k^{l-1}}$$

And,

$$\Omega = 18\zeta(l-1) - 12\zeta(l) + 2$$

This describe the probability of transformation for a cell in the middle layer. We can approximate the result over the tissue equal to this value by N/3 (middle layer) and with half contribution for the top and bottom layer resulting in

$$\Omega = 12\zeta(l-1) - 8\zeta(l) + 4/3$$

Appendix 3 – Probability of initiation (exponential function). Let's now assume the oncogenic field decays as an exponential function:

$$p_{nk} = p_{n0} e^{-(k-1)k_c^{-1}}$$

Where k_c is a decay constant expressed in terms of k-neighbourhood for simplicity. If two cells are in contact, the probability of initiation will be p_{n0} as per definition of p_{n0}. When cells are at a k_c+1 distance, this probability is 1/e lower, i.e. ~30% lower. In the case of 3D hexagonal tessellation, the factor Cp_n can be now expressed as:

$$\Omega = \sum_{k=1}^{\infty} (k^2 s_0 + 2) e^{-(k-1)k_c^{-1}}$$

Or the sum of the series:

$$\Omega = 2 \sum_{k=1}^{\infty} e^{-(k-1)k_c^{-1}} + s_0 \sum_{k=1}^{\infty} k^2 e^{-(k-1)k_c^{-1}}$$

The first series converges to:

$$\sum_{k=1}^{\infty} e^{-(k-1)k_c^{-1}} = \frac{e^{k_c^{-1}}}{e^{k_c^{-1}} - 1}$$

The second series can be represented as:

$$\sum_{k=1}^{\infty} k^2 e^{-(k-1)k_c^{-1}} = e^{k_c^{-1}} \sum_{k=1}^{\infty} k^2 e^{-k/k_c} = \frac{e^{2k_c^{-1}} \left(e^{k_c^{-1}} + 1\right)}{\left[e^{k_c^{-1}} - 1\right]^3}$$

Therefore,

$$\Omega = e^{k_c^{-1}} \frac{(2+s_0)e^{2k_c^{-1}} + (4+s_0)e^{k_c^{-1}} + 2}{\left[e^{k_c^{-1}} - 1\right]^3}$$

Therefore, Ω can be easily checked numerically. With s_0 = 6, once again to confirm mathematical consistence, small values of k_c return $\Omega \rightarrow 8$, as in the case where only adjacent cells are important. Shallower decays will again increase this value. For instance, $\Omega \sim 50$, representing the case where mutants as far as five cells, already exhibit two orders of magnitude less likelihood to contribute to transformation.

References

1. Merlo, L.M.F., Pepper, J.W., Reid, B.J. & Maley, C.C. Cancer as an evolutionary and ecological process. *Nature Reviews Cancer* **6**, 924-935 (2006).
2. Tomlinson, I.P. & Bodmer, W.F. Modelling the consequences of interactions between tumour cells. *Br J Cancer* **75**, 157-160 (1997).
3. Axelrod, R., Axelrod, D.E. & Pienta, K.J. Evolution of cooperation among tumor cells. *Proceedings of the National Academy of Sciences of the United States of America* **103**, 13474-13479 (2006).
4. Gatenby, R.A. & Vincent, T.L. Application of quantitative models from population biology and evolutionary game theory to tumor therapeutic strategies. *Mol Cancer Ther* **2**, 919-927 (2003).
5. Inda, M.D. *et al.* Tumor heterogeneity is an active process maintained by a mutant EGFR-induced cytokine circuit in glioblastoma. *Genes & Development* **24**, 1731-1745 (2010).
6. Reeves, M.Q., Kandyba, E., Harris, S., Del Rosario, R. & Balmain, A. Multicolour lineage tracing reveals clonal dynamics of squamous carcinoma evolution from initiation to metastasis. *Nat Cell Biol* **20**, 699-709 (2018).
7. Janiszewska, M. & Polyak, K. A confetti trail of tumour evolution. *Nat Cell Biol* **20**, 639-641 (2018).
8. Bonavia, R., Inda, M.D., Cavenee, W.K. & Furnari, F.B. Heterogeneity Maintenance in Glioblastoma: A Social Network. *Cancer Research* **71**, 4055-4060 (2011).
9. Marusyk, A. *et al.* Non-cell-autonomous driving of tumour growth supports sub-clonal heterogeneity. *Nature* **514**, 54-58 (2014).
10. Parsons, B.L. Many different tumor types have polyclonal tumor origin: evidence and implications. *Mutat Res* **659**, 232-247 (2008).
11. Beerenwinkel, N. *et al.* Genetic progression and the waiting time to cancer. *PLoS Comput Biol* **3**, e225 (2007).
12. Eldar, A., Rosin, D., Shilo, B.Z. & Barkai, N. Self-enhanced ligand degradation underlies robustness of morphogen gradients. *Dev Cell* **5**, 635-646 (2003).
13. Ibanes, M. & Izpisua Belmonte, J.C. Theoretical and experimental approaches to understand morphogen gradients. *Mol Syst Biol* **4**, 176 (2008).
14. Melen, G.J., Levy, S., Barkai, N. & Shilo, B.Z. Threshold responses to morphogen gradients by zero-order ultrasensitivity. *Mol Syst Biol* **1**, 2005 0028 (2005).
15. Uhlirova, M., Jasper, H. & Bohmann, D. Non-cell-autonomous induction of tissue overgrowth by JNK/Ras cooperation in a Drosophila tumor model. *Proc Natl Acad Sci U S A* **102**, 13123-13128 (2005).
16. Hanahan, D. & Folkman, J. Patterns and emerging mechanisms of the angiogenic switch during tumorigenesis. *Cell* **86**, 353-364 (1996).
17. Riedel, A., Shorthouse, D., Haas, L., Hall, B.A. & Shields, J. Tumor-induced stromal reprogramming drives lymph node transformation. *Nat Immunol* **17**, 1118-1127 (2016).

18. Tape, C.J. *et al.* Oncogenic KRAS Regulates Tumor Cell Signaling via Stromal Reciprocation. *Cell* **165**, 910-920 (2016).
19. Wu, M., Pastor-Pareja, J.C. & Xu, T. Interaction between Ras(V12) and scribbled clones induces tumour growth and invasion. *Nature* **463**, 545-548 (2010).
20. Cleary, A.S., Leonard, T.L., Gestl, S.A. & Gunther, E.J. Tumour cell heterogeneity maintained by cooperating subclones in Wnt-driven mammary cancers. *Nature* **508**, 113-117 (2014).
21. Ponomarova, O. & Patil, K.R. Metabolic interactions in microbial communities: untangling the Gordian knot. *Curr Opin Microbiol* **27**, 37-44 (2015).
22. D'Souza, G. *et al.* Ecology and evolution of metabolic cross-feeding interactions in bacteria. *Nat Prod Rep* **35**, 455-488 (2018).
23. Momeni, B., Waite, A.J. & Shou, W. Spatial self-organization favors heterotypic cooperation over cheating. *eLife* **2**, e00960 (2013).